ChemComm

Accepted Manuscript

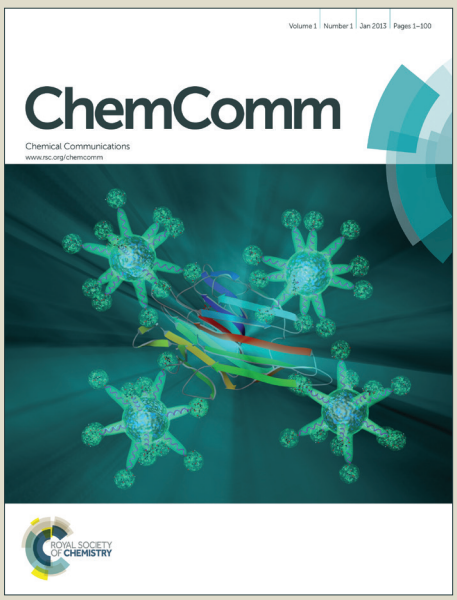

ROYAL SOCIETY OF CHEMISTRY

www.rsc.org/chemcomm

Journal Name

COMMUNICATION

Amphiphilic hollow porous shells encapsulated Au@Pd bimetal nanoparticles for aerobic oxidation of alcohols in water

Received 00th January 20xx,
Accepted 00th January 20xx

DOI: 10.1039/x0xx00000x

www.rsc.org/

Houbing Zou,[a] Runwei Wang,*[a] Jinyu Dai,[a] Yu Wang,[a] Xue Wang,[a] Zongtao Zhang,[a] and Shilun Qiu*[a]

This work describes the design, synthesis and analysis of an amphiphilic hollow mesoporous shell encapsulating catalytically active Au@Pd bimetal nanoparticle. The particle exhibited excellent catalytic activity and stability for the aerobic oxidation of primary and secondary alcohols to their corresponding aldehydes or ketones in water when using air as the oxidizing agent under atmospheric pressure.

Hollow porous shell encapsulated metal nanoparticles, also known as yolk-shell or rattle-type nanostructures, have received increasing attention and have been widely applied to important catalytic reactions,[1-3] owing to their unique structural properties, including movable core, a permeable shell and wide variability in the core and shell. The permeable shell not only allows fast diffusion of reactants and products, but also protects the catalytically active nanoparticle from sintering and provides a homogeneous micro-enviroment for the catalyst and reactants that greatly improves catalytic activity and stability.[1] Moreover, the moveable core can expose more active sites for enhancing catalytic activity. Therefore, hollow porous structures incorporated with catalytically active cores have shown promise as nanoreactors for catalysis.[3]

Currently, several synthesis strategies have been developed for designing such nanoreactors, including the Kirkendall and Ostwald ripening effects,[4] ship-in-bottle techniques,[5] bottom-up approaches using soft templating assemblies,[2,6] selective etching methods using hard templates[7] and self-templating.[8] While these methods have realized significant achievements, the shell material is still generally limited to hydrophilic silica[2,6] or hydrophobic polymer/carbon.[9] However, these shell types pose a significant limitation when applied to organic reactions in green solvent water. This is an important consideration due to environmental concerns, and has become an important research topic in the field of green catalytic chemistry.[10] While hydrophilic silica nanoreactors disperse well in water, the poor solubility of many hydrophobic substrates in water remains an important obstacle. In contrast, hydrophobic polymer/carbon nano-reactors allow the fast diffusion of reactants and products, but remain hampered by their lack of aqueous dispersibility. Therefore, constructing an amphiphilic hollow porous shell[11] that can disperse well in water yet still enrich hydrophobic substrates from aqueous solution encapsulated catalytically active core is highly desirable for developing organic reactions in solvent water.

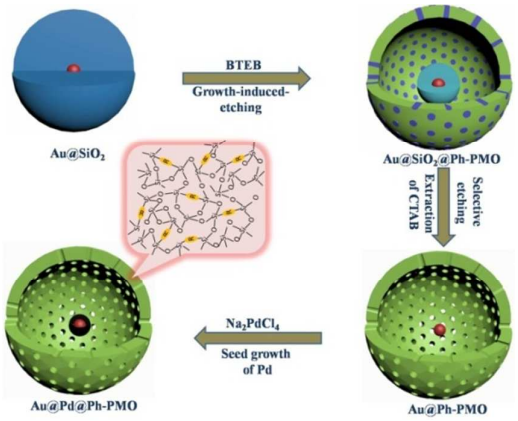

Scheme 1. Schematic illustrating the preparation of the amphiphilic nanoreactor Au@Pd@Ph-PMO.

Herein, we provide the first known design and synthesis of an amphiphilic hollow mesoporous shell encapsulating a catalytically active Au@Pd bimetal nanoparticle. First, yolk-shell structured Au@Ph-PMO nanoparticles composed of a -Ph- bridged periodic mesoporous organosilica (Ph-PMO) shell and a single Au nano-sphere core was prepared through our previous described growth-induced etching strategy.[11a] Due to the co-existence of a hydrophobic $-O_{1.5}Si-Ph-SiO_{1.5}-$unit and a hydrophilic $-SiO_2-$ unit, the obtained Au@Ph-PMO exhibited good amphiphilicity and could even serve as an excellent particle emulsifier for the formation of a Pickering emulsion. Next, Pd nanoparticles were overgrown on the surface of the Au nanosphere through a seed growth pattern to obtain the catalytically active amphiphilic nanoreactor Au@Pd@Ph-PMO. Owing to its good aqueous dispersibility and superior enriching capacity of hydrophobic substrates in water, Au@Pd@Ph-PMO

[a] State Key Laboratory of Inorganic Synthesis and Preparative Chemistry, College of Chemistry, Jilin University, 2699 Qianjin Street, Changchun, 130012, China. E-mail: rwwang@jlu.edu.cn, sqiu@jlu.edu.cn.

Electronic Supplementary Information (ESI) available: [details of any supplementary information available should be included here]. See DOI: 10.1039/x0xx00000x

exhibits excellent catalytic activity and stability for the aerobic oxidation of primary and secondary alcohols to their corresponding aldehydes and ketones in water when using air as the oxidizing agent under atmospheric pressure.

The general process for preparing the amphiphilic nanoreactor Au@Pd@Ph-PMO is illustrated in Scheme 1. A core-shell structured Au@SiO_2 particle with a diameter of 130 nm (Fig.S1a, b) is prepared through a modified Stober method. And then the Au@SiO_2 was used as a hard template for coating Ph-PMO in a basic ammonia-water-ethanol solution using CTAB (hexadecyl trimethylammonium bromide) as the surfactant. A simple process of organosilane directed growth-induced etching subsequently causes the simultaneous growth of the Ph-PMO shell and the dissolution of the silica layer, where the dissolved silica species transforms into the Ph-PMO shell through co-condensation with hydrolyzed BTEB oligomers.[11a] As show in Fig.S1f, the resulting yolk-shell structured Au@SiO_2@Ph-PMO particle has a diameter of 220 nm and a shell of 45 nm, and also contains a void space. Finally, the Au nanospheres are liberated out through selective removal of the residual SiO_2 layer, to produce the yolk-shell structured Au@Ph-PMO.

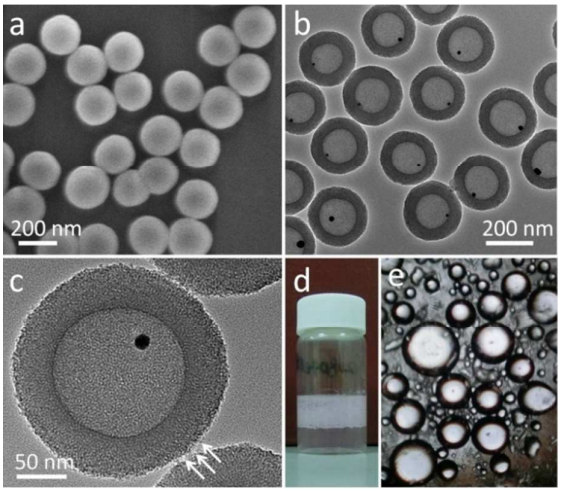

Figure.1 SEM (a), TEM (b) and high-magnification TEM (c) images of yolk-shell structured Au@Ph-PMO. (d) Digital photograph of the water in oil emulsion of the toluene-water system obtained through extracting the amphiphilic material Au@Ph-PMO in water using toluene. (e) Microphotograph of the water in oil emulsion in (d).

From the SEM image in Fig.1a, we can clearly see that Au@Ph-PMO shows uniform monodisperse spheres morphology, consisting of spheres with the same 220 nm particle diameter as Au@SiO_2@Ph-PMO. The TEM images (Fig.1b, c) further reveal the yolk-shell structure of Au@Ph-PMO, and every hollow nanosphere encapsulates only one Au nanosphere of 18-20 nm. It is notable that no external Au nanoparticles can be observed in the images, which strongly suggests that every Au@Pd bimetal nanoparticle is encapsulated by a Ph-PMO shell through the seed growth process of Pd on each Au nanoparticle. Compared with Au@SiO_2@Ph-PMO, the residual SiO_2 layer has been completely dissolved. Any residual silica fragments cannot be observed in the hollow interior of the Au@Ph-PMO particle. It is also worth mentioning that the external Ph-PMO shell, particularly its mesopore structure, is not affected at all when removing the residual SiO_2 layer using a Na_2CO_3 solution, suggesting a superior hydrothermal stability of the Ph-PMO shell that endows the amphiphilic nanoreactor Au@Pd@Ph-PMO with an excellent catalytic stability even under harsh conditions (pH > 13). Meanwhile, from the HRTEM image in Fig.1c, it is clear that the mesochannels transit into the hollow interior. This mesostructure was further confirmed by small-angle X-ray diffraction and nitrogen sorption analysis. In the small-angle XRD pattern (Fig.S2a), one sharp diffraction peak and two weak diffraction peaks appear at 2θ values of approximately 2.4, 4.4 and 4.8 degrees, indicating an ordered mesopore array in the ph-PMO shell. The nitrogen sorption isotherm (Fig.S3) shows a type IV curve with a sharp capillary condensation step in the P/P_0 range of 0.1–0.4, suggesting a uniform small mesoporous structure for Au@Ph-PMO. The corresponding Barrett–Joyner–Halenda (BJH) pore size distribution curve further confirms that the uniform mesopore size centres around 2.0 nm. The Brunauer–Emmett–Teller (BET) surface area and the total pore volume are 1182 $m^2 g^{-1}$ and 0.69 $cm^3 g^{-1}$, respectively.

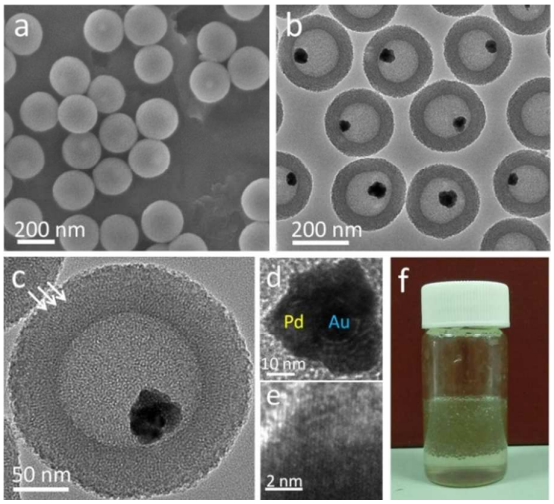

Figure.2 SEM (a), TEM (b) and high-magnification TEM (c, d, e) images of catalytically active amphiphilic nanoreactor Au@Pd@Ph-PMO. (f) Digital photograph of water in oil emulsion of the toluene-water system obtained through extracting the Au@Pd@Ph-PMO material in water using toluene.

The chemical composition of Au@Ph-PMO was characterized using solid-state ^{13}C NMR and ^{29}Si NMR spectroscopy (Fig.S4). The only appearance of resonance occurs at 133 ppm in the ^{13}C NMR spectrum, confirming the integrity of phenylene group in the Ph-PMO shell. Moreover, the ^{29}Si NMR spectrum shows the existence of both T^n and Q^n sites in the range of -50 to -70 ppm and -100 to -115 ppm, similar to our previous result,[11a] revealing the co-existence of a hydrophobic -$O_{1.5}$Si-Ph-$SiO_{1.5}$- unit and a hydrophilic -SiO_2- unit. Therefore, we anticipate that the obtained Au@Ph-PMO nanoparticle will exhibit amphiphilicity. With this characteristic, the Au@Ph-PMO can first properly disperse in water, then can form a well-defined water in oil (W/O) emulsion and aggregate at the oil–water interface when using toluene to extract the material dispersed in water, as seen in Fig.1d. It is notable that no Au@Ph-PMO material can be observed in water after extraction. The relevant optical microscopy image of W/O emulsion distinctly shows the uniform sphere morphology (Fig.1e), which is

comparable to that of a W/O emulsion using the surfactant CTAB as emulsifier (Fig.S5). These phenomena indicate that the designed Au@Ph-PMO nanoparticle is amphiphilic and can even serve as an excellent particle emulsifier for a Pickering emulsion.

After introducing palladium into the Au@Ph-PMO through a simple seed growth process, we successfully obtained the catalytically active amphiphilic nanoreactor Au@Pd@Ph-PMO. The SEM and TEM images (Fig.2a, b) reveal the same yolk-shell nanostructure, with a particle size of 220 nm and a Ph-PMO shell of 45 nm. Most importantly, all Pd nanoparticles epitaxial grew on the surface of Au nanospheres, and no extra palladium species can be observed in the Au@Pd@Ph-PMO sample. The HRTEM images (Fig.2c, d) directly reveal the core-shell structure of the Au@Pd bimetal. Moreover, the lattice fringes are clearly visible in the HRTEM image of Fig.2e, which we assign to the (111) plane of the palladium. The wide-angle XRD pattern (Fig.S6) also indicates the presence of crystalline Pd nanoparticles in the Au@Pd@Ph-PMO sample. We also analyzed the amphiphilicity of Au@Pd@Ph-PMO, and observed a similar emulsification as illustrated in Fig.2f. All these results demonstrate that the Ph-PMO hollow shell structure is not affected by the introduction of Pd.

We and others have demonstrated that amphiphilic porous nanomaterials can be viewed as excellent collectors for hydrophobic contaminant in water because they can disperse well in water yet maintain a strong affinity to hydrophobic organics.[11] In this work, we further examined the ability of such an amphiphilic hollow shell to enrich 4-methoxybenzyl alcohol in water. As shown in the Fig.S7, Au@Ph-PMO can absorb >30% of alcohol in 3 h, displaying a high sorption capacity of 1030 mg/g (0.93 mL/g), while MCM-41 only provides a sorption capacity of <100 mg/g. Notably, the sorption capacity is much higher than the total pore volume of the material (0.69 cm^3/g), suggesting that most of 4-methoxybenzyl alcohol is stored in the hollow interior of Au@Ph-PMO particles.

The selective oxidation of alcohols is one of the most important and fundamental transformations in organic synthesis and chemical industry.[12] Over the past few decades, numerous reusable metal nanoparticle-based heterogeneous catalysts have been developed and have given remarkable results.[13-15] Among them, supported Au and Pd nanoparticles have received special interest,[14] and have shown to be effective catalysts for alcohols oxidation with high

Table 1 Results of the oxidation of 4-methoxybenzyl alcohol[a]

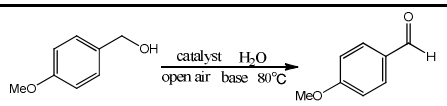

Entry	Catalyst	Conv. (%)[b]	Sel. (%)[c]
1	Pd/MCM-41	48	97
2	Au@Ph-PMO	22	98
3	Pd@Ph-PMO	67	96
4	Au@Pd@Ph-PMO	100	95
5	Au@Pd@SiO_2	72	92
6	Au@Pd@C	90	71 (29[d])

[a] Reaction condition: 4-methoxybenzyl alcohol (0.5 mmol), K_2CO_3 (0.5 mmol, 1 equi), 4 mL of H_2O, catalyst (Pd 1.5 mol%), open air, 5 h. [b, c] Catalytic reaction products were analyzed and identified by GC-MS. [d] Selectivity of 4-methoxybenzoic acid.

Table 2 Aerobic oxidation of various alcohols catalyzed by amphiphilic nanoreactor Au@Pd@Ph-PMO[a]

Entry	Substrate	Product	Time	Conv./Sel.(%)[b]
1			5 h	100/93
2	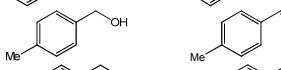		5 h	100/96
3	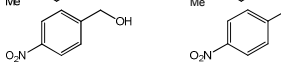		12h	56/90
4	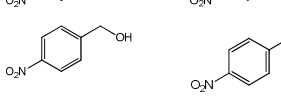		24 h	99/99
5	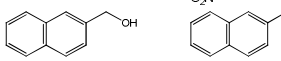		12 h	98/95
6			11 h	90/96
7	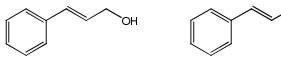		24 h	83/98
8			24 h	85/90
9[c]	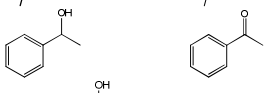		20h	>99/100
10[c]	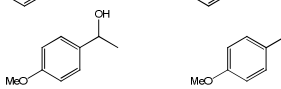		16 h	>99/100
11[c]			24 h	62/100

[a] Reaction condition: alcohol (0.5 mmol), K_2CO_3 (0.5 mmol, 1 equi), 4 mL of H_2O, catalyst (Pd 1.5 mol%), open air. [c] K_2CO_3 (1.5 mmol, 3 equi). [b] Catalytic reaction products were analyzed and identified by GC-MS.

selectivity and stability. However, there is little literature available on the aerobic oxidation of alcohols in water using air as the oxidizing agent under atmospheric pressure. Moreover, most of the catalysts can only be applied to a very limited range of substrates under such green catalytic conditions.[15] To better examine the catalytic activity of our designed amphiphilic nanoreactor, we chose the selective oxidation of 4-methoxybenzyl alcohol as the model reaction, then compared its catalytic performance with that of various hydrophilic and hydrophobic Pd-based catalysts. The results are summarized in Table 1. Under the above green catalytic condition, MCM-41 supported Pd only shows a conversion of 48%, much lower than the activity using toluene as the solvent,[14a] which can be attributed to the poor solubility and low mass transfer of hydrophobic substrate. In contrast, our designed Au@Pd@Ph-PMO catalyst gives a conversion of 100% with a selectivity of 95%, which is comparable to the activity achieved using oxygen as the oxidizing agent and an organic solvent.[14] Moreover, the yield (95%) is also obviously higher than that of nanoreactors with a hydrophilic silica shell (66%) and a hydrophobic C shell (64%). Considering their identical catalytically active site (bimetal Au@Pd), the much enhanced activity should indeed be attributed to the enrichment effect of the amphiphilic hollow Ph-PMO shell to hydrophobic substrate, and the lower selectivity of Au@Pd@C is due to the adsorption effect of porous C shell to the product aldehyde, thus leading to further oxidation.[14e] It is also worth noting that the activity of bimetal catalyst is superior to that of their monometallic counterparts, ascribed to the synergistic effects of bimetallic nanoparticles.[13c,16]

The scope of the presented catalyst system was then subsequently extended to the aerobic oxidation of a large variety of alcohols. The results summarized in Table 2 show that Au@Pd@Ph-PMO was highly active and extremely selective for the oxidation of all substrates. Primary aromatic alcohols including benzyl alcohol, substituted benzyl alcohols, 1-naphthylmethanol and heterocyclic furfuryl alcohol (entries 1–6) could all be easily oxidized to corresponding aldehydes with conversions of >90% and selectivities of >90%. It is notable that substrate in the electron-withdrawing group (entry 5, 6), when substituting an aromatic alcohol, prefers to be oxidized to its corresponding carboxylic acid. Secondary aromatic alcohols (entry 9, 10) were also effectively converted to their corresponding ketones with 100% selectivity. In addition, superior activity was achieved in the oxidation of allylic alcohols (entry 7, 8) to corresponding aldehydes. Most importantly, inert saturated secondary alcohol (entry 11), which has been reported as difficult to oxidize,[14c,e] can also be converted to its corresponding ketone at a considerable conversion rate. All these catalytic results indicate a high versatility of Au@Pd@Ph-PMO.

A typical advantage of nanoreactor catalysts is that, the leaching and sintering of catalytic active nanoparticles can be effectively prevented, thus leading to excellent catalytic stability.[1-3] The reusability of Au@Pd@Ph-PMO was tested by using 4-methoxy-benzyl alcohol as a model substrate. As shown in Fig.S8, this novel amphiphilic nanoreactor exhibits a conversion of >96% with a selectivity of >95% after ten recycling runs. The liquid phase of the reaction mixture was collected after the tenth run and analyzed by inductively coupled plasma mass spectrometry. There were no dissolved gold and palladium species detected. The catalyst was also recovered and examined after reusing ten times. Furthermore, the TEM images (Fig.S9) shows that the yolk-shell nanostructure and the active Au@Pd bimetal structure do not change. Based on these results, we can attribute the excellent catalytic activity and stability observed in these experiments to the amphiphilic property and the high hydrothermal stability of Ph-PMO hollow shell as well as the unique yolk-shell nanostructure.

In summary, we have designed a nanoreactor composed of an amphiphilic Ph-PMO hollow shell and an Au@Pd bimetal nanoparticle core. Owing to the high hydrothermal stability, the enrichment effect for hydrophobic organics in water and the unique yolk-shell nanostructure, the amphiphilic nanoreactor Au@Pd@Ph-PMO showed excellent catalytic activity and stability for aerobic oxidation of alcohols in water using air as oxidizing agent under atmospheric pressure. A wide range of substrates, including aromatic alcohols, allylic alcohols and saturated alcohol can all be effectively oxidized to corresponding aldehydes and ketones with high selectivity. Moreover, the catalyst was easily recoverable and reusable at least ten times without any loss of catalytic efficiency. Because of the flexibility of our strategy, we believe that amphiphilic hollow mesoporous shell encapsulated other metal or bimetal nanoparticle can be easily prepared for application in other organic reactions in water. Selective hydrogenation of alkyne and cinnamaldehyde in water is underway in our laboratories and results will be reported in future work.

This work was supported by National Natural Science Foundation of China (21390394), the National Basic Research Program of China (2012CB821700, 2011CB808703), NSFC (21261130584, 91022030), “111” project (B07016), Award Project of KAUST (CRG-1-2012-LAI-009) and Ministry of Education, Science and Technology Development Center Project (20120061130012).

Notes and references

1 (a) J. Liu, S. Qiao, J. Chen, X. Lou, X. Xing. G. Lu, *Chem. Commun*. 2011, **47**, 12578; (b) F. Schüth, *Chem. Mater.* 2014, **26**, 423; (c) G. Carolina, C. Baldizzone, H. Bongard, B. Spliethoff, C.Weidenthaler, J. Meier, K.Mayrhofer, F. Schüth. *Adv. Funct. Mater.* 2014, **24**, 220.
2 (a) J. Liu, S. Qiao, S. Hartono, G. Lu, *Angew. Chem. Int. Ed.* 2010, **49**, 4981; (b) J. Lee, J. Park, H. Song, *Adv. Mater.* 2008, **20**, 1523; (c) P. Arnal, M. Comotti, F. Schüth, *Angew. Chem. Int. Ed.* 2006, **45**, 8224; (d) I. Lee, J. Joo, Y. Yin, F. Zaera, *Angew. Chem. Int. Ed.* 2011, **50**, 10208.
3 (a) G. Wang, J. Hilgert, F. Richter, F. Wang, H. Bongard, B. Spliethoff, C. Weidenthaler, F. Schüth, *Nat. Mater.* 2014, **13**, 293; (b) J. Liu, H. Yang, F. Kleitz, Z. Chen, T. Yang, E. Strounina, G. Lu, S. Qiao, *Adv. Funct. Mater.* 2012, **22**, 591; (c) Y. Yang, X. Liu, X. Li, J. Zhao, S. Bai, J. Liu, Q. Yang, Angew. Chem. **2012**, 124, 9298; (d) X. Fang, Z. Liu, M. Hsieh, M. Chen, P. Liu, C. Chen, N. Zheng, *ACS Nano* 2012, **6**, 4434.
4 (a) Y. Yin, R. Rioux, C. Erdonmez, S. Hughes, G. Somorjai, A. Alivisatos, *Science* 2004, **304**, 711; (b) J. Li, H. Zeng, *J. Am. Chem. Soc.* 2007, **129**, 15839.
5 M. Xiao, C. Zhao, H. Chen, B. Yang, J. Wang, *Adv. Funct. Mater.* 2012, **22**, 4526.
6 (a) X. Wu, D. Xu, *J. Am. Chem. Soc.* 2009, **131**, 2774; (b) X. Wu, D. Xu, *Adv. Mater.* 2010, **22**, 1516.
7 (a) G. Qi, Y. Wang, L. Estevez, A. Switzer, X. Duan, X. Yang, E. Giannelis, *Chem. Mater.* 2010, **22**, 2693; (b) Y. Yang , J. Liu , X. Li , X. Liu , Q. Yang , *Chem. Mater.* 2011, **23**, 3676.
8 (a) X. Fang, X. Zhao, W. Fang, C. Chen, N. Zheng, *Nanoscale*, 2013, **5**, 2205; (b) Z. Teng, X. Su, Y. Zheng, J. Sun, G. Chen, C. Tian, J. Wang, H. Li, Y. Zhao, G. Lu, *Chem. Mater.* 2013, **25**, 98.
9 (a) B. Y. Guan, X. Wang, Y. Xiao, Y. L. Liu, Q. S. Huo, *Nanoscale* 2013, **5**, 2469; (b) N. Li, Q. Zhang, J. Liu, J. Joo, A. Lee, Y. Gan, Y. Yin, *Chem. Commun.* 2013, **49**, 5135.
10 (a) N. Isley, F. Gallou, B. Lipshutz, *J. Am. Chem. Soc.* 2013, **135**, 17707; (b) C. Deraedt, N. Pinaud, D. Astruc, *J. Am. Chem. Soc.* 2014, **136**, 12092; (c) B. Lipshutz, S. Ghorai, *Aldrichimica Acta.* 2012, **45**, 3; (d) G. Sorella, G. Strukul, A. Scarso, *Green Chem.* 2015, **17**, 644.
11 (a) H. Zou, R. Wang, X. Li, X. Wang, S. Zeng, S. Ding, L. Li, Z. Zhang, S. Qiu, *J. Mater. Chem. A,* 2014, **2,** 12403; (b) Y. Guan, X. Meng, D. Qiu, *Langmuir* 2014, **30,** 3681; (c) Y. Yang, M. Ambrogi, H. Kirmse, Y. Men, M. Antonietti, J. Yuan, *Chem. Mater.* 2015, **27,** 127.
12 R. Sheldon, J. Kochi, *Metal-Catalyzed Oxidations of Organic Compounds,* Academic Press, New York, 1981.
13 (a) N. Dimitratos, J. Lopez-Sanchez, G. Hutchings, *Chem. Sci.* 2012, **3**, 20; (b) S. Davis, M. Ide, R. Davis, *Green Chem.* 2013, **15**, 17; (c) D. Enache, J. Edwards, P. Landon, B. Solsona-Espriu, A. Carley, A. Herzing, M. Watanabe, C. Kiely, D. Knight, G. Hutchings. *Science,* 2006, **311**, 362.
14 (a) B. Karimi, S. Abedi, J. Clark, V. Budarin. Angew. Chem. Int. Ed. 2006, **45**, 4776; (b) H. Miyamura, R. Matsubara, Y. Miyazaki, S. Kobayashi, Angew. Chem. 2007, **119**, 4229; (c) G. Chen, S. Wu, H.Liu, H. Jiang, Y. Li, *Green Chem.* 2013, **15**, 230; (d) Z. Qiao, P. Zhang, S. Chai, M. Chi, G. Veith, N. Gallego, M. Kidder, S. Dai, *J. Am. Chem. Soc.* 2014, **136**, 11260; (e) J. Han, Y. Liu, R. Guo, *Adv. Funct. Mater.* 2009, **19**, 1112.
15 (a) Y. Hong, X. Yan, X. Liao, R. Li, S. Xu, L. Xiao, J. Fan, *Chem. Commun.* 2014,**50**, 9679; (b) Y. Li, Y. Gao, C. Yang, *Chem. Commun.* 2015, **51**, 7721.
16 Y. Chen, Q. Xu , S. Yu , H. Jiang, *Small* 2015, **11**, 71.